

# Features of Convective heat transfer on MHD peristaltic movement of Williamson fluid with the presence of Joule heating

Naheeda Iftikhar<sup>1</sup>, Abdul Rehman<sup>2</sup> and Muhammad Najam Khan<sup>3</sup>

<sup>1</sup>Department of Mathematics, BUITEMS, Quetta, Pakistan

<sup>2</sup>Department of Mathematics, University of Balochistan, Quetta, Pakistan

<sup>3</sup>Department of Chemical Engineering, BUITEMS, Quetta, Pakistan

Email: naheeda\_iftikhar@yahoo.com

**Abstract.** This article reflects the features of convective heat transfer with radially magnetic field of an incompressible Williamson fluid with peristaltic motion and Joule heating in a curved channel. Mathematical study has been carried out with low Reynolds number under consideration of long wavelength approximations. The system of nonlinear equations with small values of Weissenberg number has been obtained and solution of these equations has been constructed. The spectacular characteristics of flow quantities are carried out with special focus on velocity, temperature, heat transfer and trapping. It is examined that pressure gradient heightens for large values of Weissenberg number and magnetic field parameter. The velocity and temperature shows low behaviour for magnetic field parameter and moreover Weissenberg and Biot numbers has opposite effect on temperature distribution. Streamlines pattern are also represented with different parameters.

**Keywords:** Williamson fluid, peristaltic motion, Joule heating, convective boundary conditions, HPM Solution.

## 1. Introduction

Involuntary movements of the tubular circular and longitudinal muscles is the peristaltic motion, principally in the digestive tract but once in a while in other vacuous tubes of the body has made grievous attraction to the recent researchers for the expanse of this field in fluid dynamics. This development has found in Physiology; Peristalsis is an inherent property of many syncytial smooth hairs Myotubes, Simulation of some point can cause a contractile ring in the body Sphincter of the intestine, and this ring then spreads along the tube. In this way, Peristalsis occurs in gastrointestinal tract, bile ducts and other gland ducts throughout the body, the uterus and many other smooth muscle tubes of the body. One main field of application of this principle is the construction of finger pumps, rollers pumps that are used in the conveyance of liquids without the contact with the pumping machine. The very first who made the interesting attempt of research on the peristaltic flow are Latham [1] and Shapiro et al [2]. Later on a very substantial study has been reported by the theoretical and experimental approach. One can inquire elite studies [3-8] and many references there in. Besides this interest also exist in the transportation of fluid of



peristaltic MHD flow in a channel linked with some problems of conductive physiological movement of fluids e.g. motility disorders in gastrointestinal tract, Urinary tract treatment problems, Theoretical and experimental investigation on the procedure of peristaltic MHD compressor. Study also exist on Peristaltic motion of (MHD) flow of viscous and non-Newtonian fluid. Temperature and flow of heat are concerned with heat transfer mechanism [9-13]. Temperature is basically about the property of thermodynamic. It depicts the use of amount of thermal energy, while the transfer of thermal energy from one to another place is flow of heat. The major categories of heat transfer are (i) conduction (ii) convection (iii) radiation. Moreover, in the procedure of oxygenation and haemodialysis the significance of thermal effects of blood made learning about the performance of heat transfer in peristalsis.

By literature review and considering heat transfer study for the peristaltic motion of viscous and non-Newtonian fluids [14-20]. Besides the transportation of fluid in an uncoiled channel there also exist curved channels which are used for fluid flows in industry and physiological applications.

Flexibility of the walls may cause of the peristaltic flow in the channel / tube. In the present literature, useful consideration of channel is taken for the peristaltic flows. Mittra and Prasad [21] considered peristaltic motion and studied wall properties effects. Davies [22] examined flow stability with compliant walls of the plane channel. Srivastav [23] studied the peristaltic flow of the mixture of particles and fluids with wall flexibility. Haroun [24] considered an asymmetric channel for peristaltic flow and studied the effects of compliant wall. Radhakrishnamacharya [25] analysed the peristaltic transport of heat transfer with effects of flexible walls. Muthu et al. [26] examined wall properties of the micropolar fluid with peristaltic motion in a circular cylindrical tube. Another study by Elnaby [27], where he studied wall properties effects on a viscous fluid with peristaltic motion.

Hayat et al. [28-29] considered the Johnson-Segalman and Jeffery fluids with peristaltic flow and examined the influence of compliant walls respectively. The same phenomenon considered by Ali et al. [30] with Maxwell fluid in a channel. Kothandapani [31] also examined the effect of wall properties by considering MHD peristaltic flow of viscous fluid but in a porous channel. The more work has been carried out by Srinivas et al. [32] in the existence of slip effects. Srinivas [33] also considered porous space and examined the effect of compliant walls on MHD peristaltic flow. Hayat and Hina [34] analyzed the effect of compliant walls by considering Maxwell fluid.

In view of literature cited above, it is cleared that insufficient studies have been done with curved channel on the peristaltic mechanism. Sato et al. [35] discussed peristaltic motion in a curved channel due to transverse rebounds of the walls. [36] Ali et al carried out analytical study of long wavelength approximation in a curved channel and peristaltic motion. Ali et al. [37-38] extended the investigation of ref. [34] for heat transfer characteristics of third grade fluid. Hayat et al. [39] studied Newtonian fluid with peristaltic motion with effect of compliant walls in a curved channel. This study is extended by himself [40] and Hina et al. [41] for third-grade and Johnson-Segalman fluids. The joint effect of heat and mass transfer with peristaltic flow of Johnson-Segalman fluid was studied by Hina et al. [42]. Author also discussed effect of wall properties with peristaltic motion of pseudoplastic fluid in a curved channel [43]. Another study [44] the slip effects of third grade fluid with the peristaltic transport. And Finally, [45] carried out numerical study of nanofluid with peristaltic motion in a curved channel. Few studies associated with our discussion are [46-49].

The present investigation based on the study of Williamson fluid with peristaltic flow and effects of radially magnetic field with analysis of convective heat transfer. Williamson fluid is the generalization of non-Newtonian fluid model. For the better understanding of the investigation, four main sections are developed. First section comprises of problem formulation under consideration of non-dimensional governing equations with geometry of the problem and convective boundary conditions in wave frame. Second section gives the solution of considered problem with large number of constants. Section three shows the graphical

results of emerging parameters on velocity, temperature, pressure gradient and coefficient of heat transfer and trapping phenomenon has also visualized in this section. And finally conclusion has summarized in last fourth section.

## 2. Formulation of the problem

The Peristaltic wave of an electrically conducting non-Newtonian incompressible substance in a curved channel of  $L^*$  with unvarying broadness  $2a_0$  coiled in a circle with centre at  $o'$  is considered. By choosing a curvilinear coordinate system  $(\hat{G}, \hat{L})$  with unmoving frame and the circulization of wave along the  $\hat{G}$  coordinate and  $\hat{L}$ —coordinate is in normal direction of the flow. In laboratory frame of reference, the velocity components are  $\hat{W}_1$  and  $\hat{W}_2$  in radial ( $\hat{L}$ ) and axial ( $\hat{G}$ ) direction respectively. The radial magnetic field of force  $\tilde{B}_0$  is subjected to the fluid and heat transfer is directed by the convective conditions at the walls of the channel.

Along the channel walls the motion of fluid is derived by sinusoidal wave circulating with uniform speed  $C_0$ . Mathematically we will have

$$\hat{H}(\hat{G}, \hat{t}) = - \left[ a_{00} + a_{11} \text{Si} n \left( \frac{2\pi'}{c_0} (\hat{G} - \lambda c_0 \hat{t}) \right) \right] \quad (1)$$

In this equation  $c_0$  refers the speed,  $a_{11}$  is amplitude,  $\lambda c_0$  is wave length and  $\tilde{t}$  is time of the wave in unmoving frame. The velocity

$$\hat{\mathbf{W}} = (\hat{W}_1(\hat{G}, \hat{L}, \hat{t}), \hat{W}_2(\hat{G}, \hat{L}, \hat{t}), 0) \quad (2)$$

$$\hat{\tau} = -[\eta'_{\infty} + (\eta'_0 - \eta'_{\infty})(1 + \Gamma'|\dot{\gamma}'|)]\dot{\gamma}' \quad (3)$$

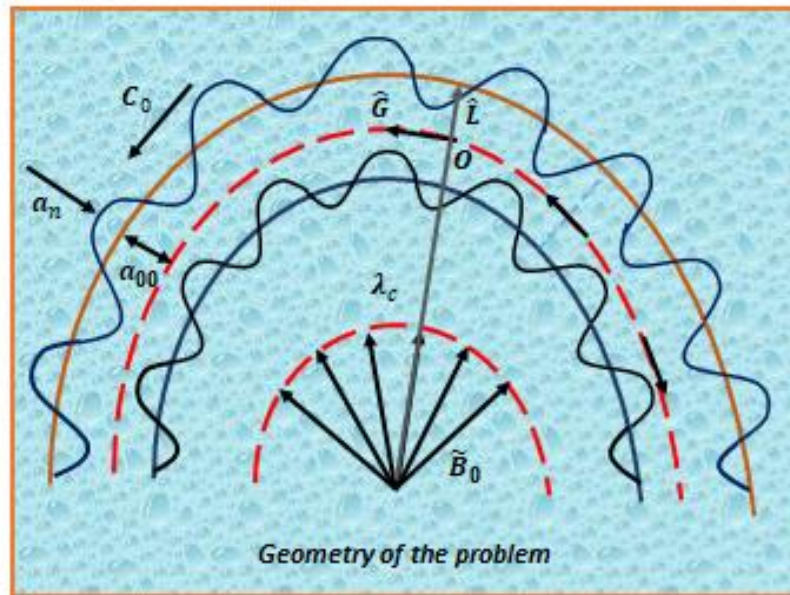


Figure 1. Geometry of the flow

$$\dot{\gamma}' = \sqrt{\frac{1}{2} \sum_j \sum_m \dot{\gamma}'_{jm} \dot{\gamma}'_{mj}} = \sqrt{\frac{\pi'}{2}}. \quad (4)$$

Where  $\pi'$  refers the second unvarying tensor. The constitutional equation for the case of  $\eta'_\infty = 0$  bring down

$$\hat{\tau} = -\eta'_0 [ + (\eta'_0 - \eta'_\infty) (1 + \Gamma' |\dot{\gamma}'|) ] \dot{\gamma}' \quad (5)$$

In the laboratory frame, the governing equation for the motion of fluid are given by

$$\frac{\partial}{\partial \hat{L}} \{ (L^{**} + \hat{L}) \hat{W}_1 \} + L^{**} \left( \frac{\partial \hat{W}_2}{\partial \hat{G}} \right) = 0, \quad (6)$$

$$\rho' \left[ \frac{\partial \hat{W}_1}{\partial \hat{t}} + \hat{W}_1 \left( \frac{\partial \hat{W}_1}{\partial \hat{L}} \right) + L^{**} \left( \frac{\hat{W}_2}{L^{**} + \hat{L}} \right) \frac{\partial \hat{W}_1}{\partial \hat{G}} - \left( \frac{\hat{W}_2^2}{L^{**} + \hat{L}} \right) \right] = - \frac{\partial \hat{P}}{\partial \hat{L}} + \frac{1}{(L^{**} + \hat{L})} \frac{\partial}{\partial \hat{L}} \{ (L^{**} + \hat{L}) \hat{\tau}_{\hat{L}\hat{L}} \} + \left( \frac{L^{**}}{L^{**} + \hat{L}} \right) \frac{\partial \hat{\tau}_{\hat{L}\hat{G}}}{\partial \hat{G}} - \frac{\hat{\tau}_{\hat{G}\hat{G}}}{(L^{**} + \hat{L})} \quad (7)$$

$$\rho' \left[ \frac{\partial \hat{W}_2}{\partial \hat{t}} + \hat{W}_1 \left( \frac{\partial \hat{W}_2}{\partial \hat{L}} \right) + L^{**} \left( \frac{\hat{W}_2}{L^{**} + \hat{L}} \right) \left( \frac{\partial \hat{W}_2}{\partial \hat{G}} \right) - \hat{W}_1 \left( \frac{\hat{W}_2}{L^{**} + \hat{L}} \right) \right] = \left( \frac{L^{**}}{L^{**} + \hat{L}} \right) \frac{\partial \hat{P}}{\partial \hat{G}} +$$

$$\left( \frac{1}{(L^{**} + \hat{L})^2} \right) \frac{\partial}{\partial \hat{L}} \{ ((L^{**} + \hat{L})^2) \hat{\tau}_{\hat{L}\hat{G}} \} + \left( \frac{L^{**}}{L^{**} + \hat{L}} \right) \frac{\partial \hat{\tau}_{\hat{G}\hat{G}}}{\partial \hat{G}} - \sigma B_0^2 \hat{W}_2 / (L^{**} + \hat{L})^2 \quad (8)$$

$$\begin{aligned} \rho' c'_p \left[ \frac{\partial \hat{T}}{\partial \hat{t}} + \hat{W}_1 \left( \frac{\partial \hat{T}}{\partial \hat{L}} \right) + \hat{W}_2 \frac{L^{**}}{L^{**} + \hat{L}} \frac{\partial \hat{T}}{\partial \hat{G}} \right] &= k' \left[ \left( \frac{\partial^2 \hat{T}}{\partial \hat{L}^2} \right) + \frac{1}{L^{**} + \hat{L}} \left( \frac{\partial \hat{T}}{\partial \hat{L}} \right) + \frac{L^{**2}}{(L^{**} + \hat{L})^2} \left( \frac{\partial^2 \hat{T}}{\partial \hat{G}^2} \right) \right] \\ + \mu_0 \left[ \left( \frac{\partial \hat{W}_2}{\partial \hat{L}} - \frac{\hat{W}_2}{(L^{**} + \hat{L})} + \frac{L^{**}}{(L^{**} + \hat{L})} \left( \frac{\partial \hat{W}_1}{\partial \hat{G}} \right) \right) \hat{\tau}_{\hat{L}\hat{G}} + \left( \frac{\partial \hat{W}_2}{\partial \hat{L}} \right) (\hat{\tau}_{\hat{L}\hat{L}} - \hat{\tau}_{\hat{G}\hat{G}}) \right] \end{aligned} \quad (9)$$

With

$$\hat{\tau}_{\hat{G}\hat{G}} = -2\mu_0\eta_0 \left[ 1 + \Gamma' |\dot{\gamma}'| \right] \left( \frac{L^{**}}{(L^{**} + \hat{L})} \left( \frac{\partial \hat{W}_2}{\partial \hat{G}} \right) + \frac{\hat{W}_1}{(L^{**} + \hat{L})} \right), \quad (10)$$

$$\hat{\tau}_{\hat{L}\hat{G}} = \mu_0\eta_0 \left[ 1 + \Gamma' |\dot{\gamma}'| \right] \left( \frac{\partial \hat{W}_2}{\partial \hat{L}} + \frac{L^{**}}{(L^{**} + \hat{L})} \left( \frac{\partial \hat{W}_1}{\partial \hat{G}} \right) - \frac{\hat{W}_2}{(L^{**} + \hat{L})} \right), \quad (11)$$

$$\hat{\tau}_{\hat{L}\hat{L}} = -2\mu_0\eta_0 \left[ 1 + \Gamma' |\dot{\gamma}'| \right] \left( \frac{\partial \hat{W}_1}{\partial \hat{L}} \right). \quad (12)$$

Here  $\hat{P}$  refers the pressure,  $\rho'$  is fluid density,  $c'_p$  is specific heat,  $\hat{t}$  is time,  $\hat{k}$  is thermal conductivity and  $\hat{T}$  is the temperature of fluid. Unsteady flow is reasoned in unmoving frame  $(\hat{G}, \hat{L})$  whereas in moving frame  $(\hat{g}, \hat{l})$  the flow in the channel can be reasoned as steady flow.

The heat transfers because of convective cooling at the boundaries proceeds

$$\begin{aligned} \hat{k} \frac{\partial \hat{T}}{\partial \hat{L}} &= -\hat{\eta}_1 (\hat{T} - \hat{T}_0) \text{ at } \hat{L} = \hat{\eta} \\ \hat{k} \frac{\partial \hat{T}}{\partial \hat{L}} &= -\hat{\eta}_2 (\hat{T} - \hat{T}_0) \text{ at } \hat{L} = -\hat{\eta} \end{aligned} \quad (13)$$

By Preceding a wave frame  $(\hat{g}, \hat{l})$  with wave moving with speed  $c_0$  departed from the fixed frame  $(\hat{G}, \hat{L})$  by the transformations

$$\hat{g} = \hat{G} - c_0 \hat{t}, \quad \hat{l} = \hat{L}, \quad \hat{w}_1(\hat{g}, \hat{l}) = \hat{W}_1(\hat{G}, \hat{L}, \hat{t}), \quad \hat{w}_2(\hat{g}, \hat{l}) = \hat{W}_2(\hat{G}, \hat{L}, \hat{t}) - c_0, \quad (14)$$

$$\hat{T}(\hat{g}, \hat{l}) = \hat{T}(\hat{G}, \hat{L}, \hat{t}), \quad \hat{p}(\hat{g}, \hat{l}) = \hat{P}(\hat{G}, \hat{L}, \hat{t})$$

And equations (6) -(12) yields

$$\begin{aligned} \frac{\partial}{\partial \hat{l}} \{ (L^{**} + \hat{l}) \hat{w}_1 \} + L^{**} \left( \frac{\partial \hat{w}_2}{\partial \hat{g}} \right) &= 0, \\ \rho' \left[ \hat{w}_1 \left( \frac{\partial \hat{w}_1}{\partial \hat{l}} \right) + \frac{L^{**} (\hat{w}_2 + c_0)}{(L^{**} + \hat{l})} \left( \frac{\partial \hat{w}_1}{\partial \hat{g}} \right) - \frac{(\hat{w}_2 + c_0)^2}{(L^{**} + \hat{l})} \right] &= -\frac{\partial \hat{P}'}{\partial \hat{l}} + \frac{1}{(L^{**} + \hat{l})} \frac{\partial}{\partial \hat{l}} \{ (L^{**} + \hat{l}) \hat{\tau}_{\hat{l}\hat{l}} \} \end{aligned} \quad (15)$$

$$+ \left( \frac{L^{**}}{L^{**} + \hat{l}} \right) \frac{\partial \hat{\tau}_{\hat{l}\hat{g}}}{\partial \hat{g}} - \frac{\hat{\tau}_{\hat{g}\hat{g}}}{(L^{**} + \hat{l})} \quad (16)$$

$$\rho' \left[ -c_0 \left( \frac{\partial \hat{w}_2}{\partial \hat{g}} \right) + \hat{w}_1 \left( \frac{\partial \hat{w}_2}{\partial \hat{l}} \right) + \frac{L^{**}(\hat{w}_2 + c_0)}{(L^{**} + \hat{l})} \left( \frac{\partial \hat{w}_2}{\partial \hat{g}} \right) - \frac{\hat{w}_1 \hat{w}_2}{(L^{**} + \hat{l})} \right] = - \left( \frac{L^{**}}{L^{**} + \hat{l}} \right) \frac{\partial P'}{\partial \hat{g}} + \frac{1}{(L^{**} + \hat{l})^2} \frac{\partial}{\partial \hat{l}} \{ (L^{**} + \hat{l})^2 \hat{\tau}_{\hat{l}\hat{g}} \} \\ + \left( \frac{L^{**}}{L^{**} + \hat{l}} \right) \frac{\partial \hat{\tau}_{\hat{g}\hat{g}}}{\partial \hat{g}} - \frac{\sigma B_0^2 (\hat{w}_2 + c_0)}{(L^{**} + \hat{l})} \quad (17)$$

$$\rho' c'_p \left[ \frac{\partial \hat{T}}{\partial \hat{g}} + \hat{w}_1 \left( \frac{\partial \hat{T}}{\partial \hat{l}} \right) + \frac{L^{**}(\hat{w}_2 + c_0)}{L^{**} + \hat{l}} \left( \frac{\partial \hat{T}}{\partial \hat{g}} \right) \right] = \hat{k} \left[ \frac{\partial^2 \hat{T}}{\partial \hat{l}^2} + \frac{1}{L^{**} + \hat{l}} \left( \frac{\partial \hat{T}}{\partial \hat{l}} \right) + \left( \frac{L^{**}}{L^{**} + \hat{l}} \right) \frac{\partial^2 \hat{T}}{\partial \hat{g}^2} \right] +$$

$$\mu_0 \left[ \left( \frac{\partial \hat{w}_2}{\partial \hat{l}} - \frac{(\hat{w}_2 + c_0)}{(L^{**} + \hat{l})} + \frac{L^{**}}{(L^{**} + \hat{l})} \frac{\partial \hat{w}_1}{\partial \hat{g}} \right) \hat{\tau}_{\hat{l}\hat{g}} + \frac{\partial \hat{w}_2}{\partial \hat{l}} (\hat{\tau}_{\hat{l}\hat{l}} - \hat{\tau}_{\hat{g}\hat{g}}) \right] \quad (18)$$

$$\hat{\tau}_{\hat{g}\hat{g}} = -2\mu_0 \eta'_0 [1 + \Gamma' |\dot{\gamma}'|] \left( \frac{L^{**}}{(L^{**} + \hat{l})} \frac{\partial (\hat{w}_2 + c_0)}{\partial \hat{g}} + \frac{\hat{w}_1}{(L^{**} + \hat{l})} \right) \quad (19)$$

$$\hat{\tau}_{\hat{l}\hat{g}} = \mu_0 \eta'_0 [1 + \Gamma' |\dot{\gamma}'|] \left( \frac{\partial \hat{w}_2}{\partial \hat{l}} + \frac{L^{**}}{(L^{**} + \hat{l})} \frac{\partial \hat{w}_1}{\partial \hat{g}} - \frac{\hat{w}_2}{(L^{**} + \hat{l})} \right) \quad (20)$$

$$\hat{\tau}_{\hat{l}\hat{l}} = -2\mu_0 \eta'_0 [1 + \Gamma' |\dot{\gamma}'|] \left( \frac{\partial \hat{w}_1}{\partial \hat{l}} \right) \quad (21)$$

By defining

$$g' = \frac{2\pi \hat{g}}{\lambda_{c_0}}, \quad l' = \frac{\hat{l}}{a_{00}}, \quad \hat{w}_1 = \frac{\hat{w}_1}{c_0}, \quad \hat{w}_2 = \frac{\hat{w}_2}{c_0}, \quad \hat{\delta} = \frac{2\pi' a_{00}}{\lambda_{c_0}}, \quad \hat{\eta} = + \frac{\hat{\mathbf{H}}}{a_{00}}, \quad P' = \frac{2\pi a_{00}^2 \hat{p}}{c_0 \mu_0 \lambda_{c_0}}, \quad W'_e = \frac{\Gamma' c_0}{a_{00}}, \\ M' = \left( \frac{\sigma'}{\mu_0} \right)^{1/2} \tilde{B}_0 a_{00}, \quad \text{Re} = \frac{\rho' c_0 a_{00}}{\mu_0}, \quad \hat{k} = \frac{L^{**}}{a_{00}}, \quad P_r = \frac{\mu_0 c'_p}{\hat{k}}, \quad \hat{t} = \frac{c_0 \hat{t}}{\lambda_{c_0}}, \quad \hat{\theta} = \frac{\hat{T} - \hat{T}_0}{\hat{T}_0}, \\ E'_c = \frac{c_0^2}{T'_0 c_p}, \quad \hat{B}_r = P_r E'_c \quad (22)$$

$$\hat{w}_1 = \hat{\delta} \frac{\hat{k}}{l' + \hat{k}} \frac{\partial \Omega}{\partial g'}, \quad \hat{w}_2 = - \frac{\partial \Omega}{\partial l'} \quad (23)$$

Equation (10) fulfilled and former expressions under wavelength and low Reynolds number come down to

$$\frac{dP'}{dl'} = 0, \quad (24)$$

$$\frac{\hat{k}}{l' + \hat{k}} \frac{dP'}{dg'} = \frac{1}{(l' + \hat{k})^2} \frac{\partial}{\partial l'} \left\{ (l' + \hat{k})^2 \hat{\tau}_{l'g} \right\} - \frac{M'}{(l' + \hat{k})^2} \left( 1 - \frac{\partial \Omega}{\partial l'} \right),$$

$$(25) \quad \frac{\partial^2 \hat{\theta}}{\partial l'^2} + \frac{1}{l' + \hat{k}} \frac{\partial \hat{\theta}}{\partial l'} + B'_r \left[ \left( \frac{\partial^2 \Omega}{\partial l'^2} - \frac{1 - \frac{\partial \Omega}{\partial l'}}{l' + \hat{k}} \right) \hat{\tau}_{l'g} \right] = 0.$$

(26)

$$\hat{\tau}_{l'g} = \left[ 1 + W'_e \left( -\frac{\partial^2 \Omega}{\partial l'^2} - \frac{1 - \frac{\partial \Omega}{\partial l'}}{l' + \hat{k}} \right) \right] \left( -\frac{\partial^2 \Omega}{\partial l'^2} - \frac{1 - \frac{\partial \Omega}{\partial l'}}{l' + \hat{k}} \right), \quad (27)$$

Where dimensionless boundary conditions are

$$\Omega = -\frac{\hat{F}}{2}, \quad \Omega_{l'} = 1, \quad \hat{\theta}' + \hat{\beta}_1 \hat{\theta} = 0 \quad \text{at } l' = +\eta', \quad (28)$$

$$\Omega = -\frac{\hat{F}}{2}, \quad \Omega_{l'} = 1, \quad \hat{\theta}' + \hat{\beta}_1 \hat{\theta} = 0 \quad \text{at } l' = -\eta'.$$

$$\eta(\hat{g}) = [1 + \varepsilon \sin(2\pi \hat{g})] \quad (29)$$

Whereas  $\hat{\beta}_1 = \frac{\eta'_d}{\hat{k}}$  and  $\hat{\beta}_2 = \frac{\eta'_d}{\hat{k}}$  refers the Biot numbers at the upper and lower walls.

Coefficient of heat transfer is defined as

$$Z' = \eta'_g \hat{\theta}'(\eta'). \quad (30)$$

### 3. Solution Methodology

By letting

$$\begin{aligned} \Omega &= \Omega_0 + \hat{W}_e \Omega_1, \dots, \\ \hat{\tau}_{l'g} &= \hat{\tau}_{0l'g} + \hat{W}_e \hat{\tau}_{1l'g}, \dots, \\ \frac{dP'}{dg'} &= \frac{dP'_0}{dg'} + \hat{W}_e \frac{dP'_1}{dg'}, \dots, \\ \hat{\theta} &= \hat{\theta}_0 + \hat{W}_e \hat{\theta}_1, \dots, \\ \hat{F} &= \hat{F}_0 + \hat{W}_e \hat{F}_1, \dots \end{aligned} \quad (31)$$

For the solution system of zeroth and first order are

#### Zeroth order system

$$\frac{\hat{k}}{l' + \hat{k}} \frac{dP'_0}{dg'} = \frac{1}{(l' + \hat{k})^2} \frac{\partial}{\partial l'} \left\{ (l' + \hat{k})^2 \hat{\tau}_{0l'g} \right\} - \frac{M'}{(l' + \hat{k})^2} \left( 1 - \frac{\partial \Omega_0}{\partial l'} \right), \quad (32)$$

$$(33) \quad \frac{\partial^2 \hat{\theta}_0}{\partial l'^2} + \frac{1}{l' + \hat{k}} \frac{\partial \hat{\theta}_0}{\partial l'} + \hat{B}_r \left[ \left( \frac{\partial^2 \Omega_0}{\partial l'^2} - \frac{1 - \frac{\partial \Omega_0}{\partial l'}}{l' + \hat{k}} \right) \hat{\tau}_{0l'g} \right] = 0$$

$$\hat{\tau}_{0l'g'} = \left[ 1 + W'_e \left( -\frac{\partial^2 \Omega_0}{\partial l'^2} - \frac{1 - \frac{\partial \Omega_0}{\partial l'}}{l' + \hat{k}} \right) \right] \left( -\frac{\partial^2 \Omega_0}{\partial l'^2} - \frac{1 - \frac{\partial \Omega_0}{\partial l'}}{l' + \hat{k}} \right) \quad (34)$$

$$\Omega_0 = -\frac{\hat{F}_0}{2}, \quad \Omega_{0l'} = 1, \quad \theta_{0l'} + \hat{\beta}_1 \hat{\theta}_0 = 0 \quad \text{at } l' = +\eta', \quad (35)$$

$$\Omega_0 = -\frac{\hat{F}_0}{2}, \quad \Omega_{0l'} = 1, \quad \theta_{0l'} + \hat{\beta}_1 \hat{\theta}_0 = 0 \quad \text{at } l' = -\eta'$$

### First order system

$$\frac{\hat{k}}{l' + \hat{k}} \frac{dP'_1}{dg'} = \frac{1}{(l' + \hat{k})^2} \frac{\partial}{\partial l'} \left\{ (l' + \hat{k})^2 \hat{\tau}_{1l'g'} \right\} - \frac{M'}{(l' + \hat{k})^2} \left( 1 - \frac{\partial \Omega_1}{\partial l'} \right), \quad (36)$$

$$\frac{\partial^2 \hat{\theta}_1}{\partial l'^2} + \frac{1}{l' + \hat{k}} \frac{\partial \hat{\theta}_1}{\partial l'} + B'_r \left[ \left( \frac{\partial^2 \Omega_1}{\partial l'^2} - \frac{1 - \frac{\partial \Omega_1}{\partial l'}}{l' + \hat{k}} \right) \hat{\tau}_{1l'g'} \right] = 0 \quad (37)$$

$$\hat{\tau}_{1l'g'} = - \left[ \left( \frac{\partial^2 \Omega_1}{\partial l'^2} - \frac{1 - \frac{\partial \Omega_1}{\partial l'}}{l' + \hat{k}} \right) + \left( -\frac{\partial^2 \Omega_0}{\partial l'^2} - \frac{1 - \frac{\partial \Omega_0}{\partial l'}}{l' + \hat{k}} \right)^2 \right] \quad (38)$$

$$\Omega_1 = -\frac{\hat{F}_1}{2}, \quad \Omega_{1l'} = 0, \quad \hat{\theta}_{1l'} + \hat{\beta}_1 \hat{\theta}_1 = 0 \quad \text{at } l' = +\eta', \quad (39)$$

$$\Omega_1 = -\frac{\hat{F}_1}{2}, \quad \Omega_{1l'} = 0, \quad \hat{\theta}_{1l'} - \hat{\beta}'_1 \hat{\theta}_1 = 0 \quad \text{at } l' = +\eta'. \quad (40)$$

Solution obtained for the zeroth and first order systems are

$$\Omega_0 = C_1 (l' + \hat{k})^{M'} + C_2 (l' + \hat{k})^{-M'} - \frac{(l' + \hat{k})^2 \frac{dP'_0}{dg'}}{2(4 - M'^2)} - \frac{\hat{k}^3 \frac{dP'_0}{dg'}}{M'^2} + l', \quad (41)$$

$$\Omega_1 = a_{11} + \left( \frac{dP'_0}{dg'} \right)^2 a_{20} + a_{13} + a_{14} + \frac{dP'_0}{dg'} [a_{19} + a_{21} + a_{22}] - a_{15} - \frac{2(l' + \hat{k})}{1 - M'^2} + a_{16} - a_{17} + a_{18} - \frac{4}{M'^2} - \frac{dP'_1}{dg'} a_{23}, \quad (42)$$

$$\theta_0 = C_5 + C_6 \ln(l' + \hat{k}) - B'_r \left[ \frac{dP'_0}{dg'} b_{22} - b_{11} + b_{12} + b_{13} \frac{dP'_0}{dg'} (b_{20} + b_{21}) + b_{14} - b_{15} + b_{16} - b_{17} - b_{18} + \frac{2 \left( \frac{dP'_0}{dg'} \right)^2 (l' + \hat{k})^3}{9(4 - M'^2)} - b_{19} \right] \quad (43)$$

$$\theta_1 = f_1 + f_2 \ln(l' + \hat{k}) + B'_r \left[ \frac{dP'_0}{dg'} (c_{11} + c_{12} + c_{16}) + \left( \frac{dP'_0}{dg'} \right)^2 (c_{13} + c_{14} - c_{17}) + \left( \frac{dP'_0}{dg'} \right)^3 c_{15} + \frac{dP'_1}{dg'} c_{18} + c_{19} \right. \\ \left. + \frac{dP'_0}{dg'} \frac{dP'_1}{dg'} \left( -\frac{5(l' + \hat{k})^2}{32} + \frac{(l' + \hat{k})^3}{16} \right) - 2C_1 (\ln(l' + \hat{k}))^2 + \frac{5C_2 (\ln(l' + \hat{k}))^2}{4} \right] \quad (44)$$



$$\begin{aligned}
C_1 &= \frac{-(\hat{k} + \eta')^{-M'} \left( \frac{\bar{F}_0}{2} + \frac{\hat{k}^3 \frac{dP_0}{dg'}} + \frac{\frac{dP_0}{dg'} (\hat{k} - \eta')^2}{2(4 - M'^2)} + \eta' \right) + (\hat{k} - \eta')^{-M'} \left( \frac{-\bar{F}_0}{2} + \frac{\hat{k}^3 \frac{dP_0}{dg'}} + \frac{\frac{dP_0}{dg'} (\hat{k} + \eta')^2}{2(4 - M'^2)} - \eta' \right)}{(\hat{k} - \eta')^{M'} (\hat{k} + \eta')^{-M'} - (\hat{k} - \eta')^{-M'} (\hat{k} + \eta')^{M'}} \\
C_2 &= \frac{(\hat{k} + \eta')^{M'} \left( \frac{-\bar{F}_0}{2} + \frac{\hat{k}^3 \frac{dP_0}{dg'}} + \frac{\frac{dP_0}{dg'} (\hat{k} + \eta')^2}{2(4 - M'^2)} - \eta' \right) + (\hat{k} + \eta')^{2M'} \left( -(\hat{k} + \eta')^{-M'} \left( \frac{\bar{F}_0}{2} + \frac{\hat{k}^3 \frac{dP_0}{dg'}} + \frac{\frac{dP_0}{dg'} (\hat{k} - \eta')^2}{2(4 - M'^2)} + \eta' \right) + (\hat{k} - \eta')^{-M'} \left( \frac{-\bar{F}_0}{2} + \frac{\hat{k}^3 \frac{dP_0}{dg'}} + \frac{\frac{dP_0}{dg'} (\hat{k} + \eta')^2}{2(4 - M'^2)} - \eta' \right) \right)}{(\hat{k} - \eta')^{M'} (\hat{k} + \eta')^{-M'} - (\hat{k} - \eta')^{-M'} (\hat{k} + \eta')^{M'}}
\end{aligned} \tag{45}$$

#### 4. RESULTS AND DISCUSSION

This segment has developed to attain and show the phenomenon of distinct physical deeply involved parameters on velocity, temperature, pressure gradient, coefficient of flow of heat and stream function respectively. For excellence output of the existing study there is a sectional distribution of this discussion which has clear picture of graphical results.

##### (i) Velocity distribution

In this segment the conduct of velocity dispersion in curved channel for assorted parameters is depicted over figures. It is visible that velocity dispersion has opposite manner, at the walls of the channel for different valued of  $W_e'$  (Weissenberg number) and  $M'$  (Magnetic field). Observations clearly showed that velocity is less for viscous substance in comparison with Williamson fluid at lower wall, whereas it heightens at upward wall of the channel. Figure 2. (a) exhibit that there does not exist symmetry of the velocity dispersion through curvature. Effects of magnitude field (radial)  $M'$  is pictured in Figure 2. (b). It is resulted that magnetic field (radial) has opposing behavior for velocity. In the case, when magnetic field increases in magnitude the resulting situation is the gradually decrease in the flow velocity due to prejudicial effect of the electromagnetic body force. In addition, for higher values of  $M'$  Substantial reduction has been seen in the flow velocity closest to the centre of the curved channel inspite the near of the walls.

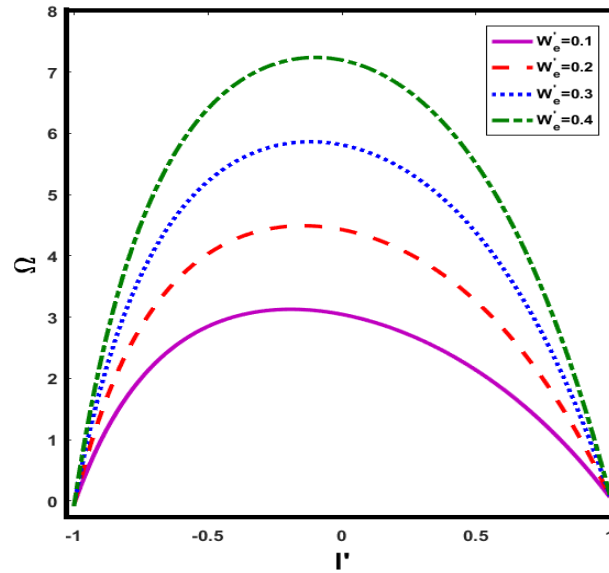


Figure 2. (a) Behavior of velocity distribution for  $W'_e$  and  $M'=4.0$ ,  $\hat{k}=2.5$ ,  $\varepsilon'=0.01$ ,  $g'=0.0$

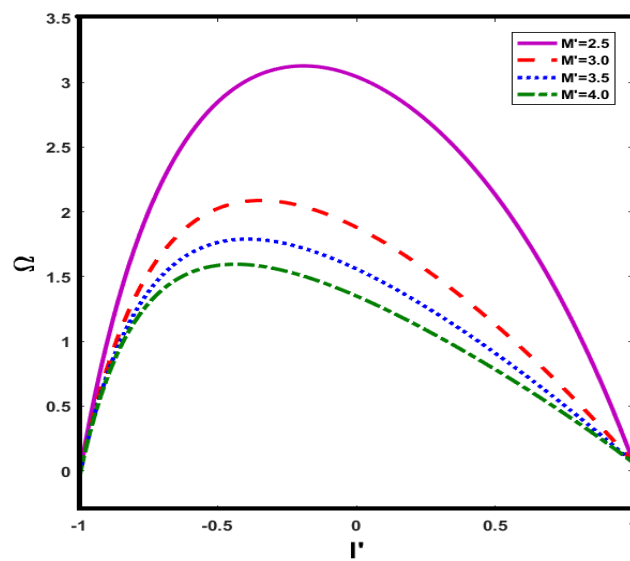


Figure 2. (b) Behavior of velocity distribution for  $M'$  and  $W'_e=0.1$ ,  $\hat{k}=2.5$ ,  $\varepsilon'=0.01$ ,  $g'=0.0$

## (ii) Temperature distribution

Visibility of temperature attributes for  $W'_e$  (Weissenberg number) and  $M'$  (Magnetic parameter) are drawn and talk about them in the Figures 3. (a) - Figure 3. (f), Figure 3. (a) represents that temperature rises for Williamson fluid (when  $W'_e \neq 0$ ). One another thing for noticing that for Williamson fluid there is less resistance in temperature dispersion near the lower wall when compared to viscous material. Figure 3. (b) and Figure 3. (c) shows the behaviour that temperature is increasing due to viscous dissipation effects while increasing Brashof number and Magnetic field parameter. Actually viscosity assists kinetic energy of the motion of the fluid particles and change into internal energy which raise the temperature distributions.

In Figure 3. (d) it is cleared that for the higher values of  $\hat{k}$  (curvature parameter) the temperature dispersion reduces. Another observation resulted that magnetic parameter  $M'$  (radial) has resistivity impact on temperature and it decreases with increasing  $M'$ . In early discussions it is observed that temperature is anti-symmetric for large values of  $\hat{k}$  in curved channel whereas it is symmetric for small values of  $\hat{k}$  in unbent channel. Figure 3. (b) illustrates that temperature distribution shows increase while increasing Brashof number. And Figure 3. (e) and Figure 3. (f) is prominently showing that  $\beta'_1$  and  $\beta'_2$  gives opposite behaviour on temperature profile in comparison on other parameters.

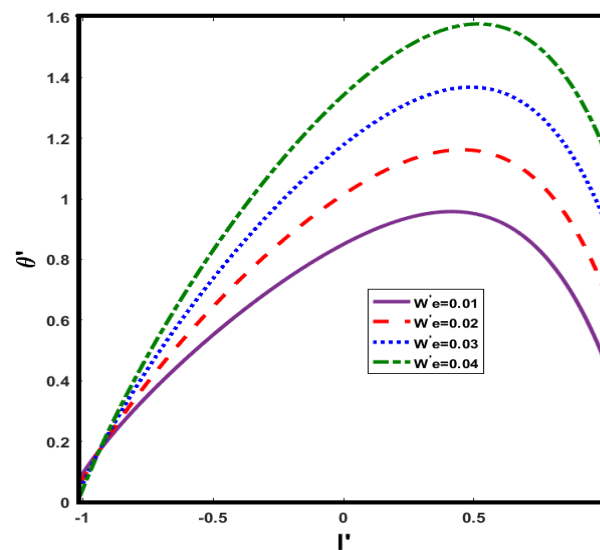


Figure 3. (a) Behavior of Temperature distribution for  $W'_e$  and  $M'=3.5$ ,  $\varepsilon'=0.1$ ,  $B'_r=0.1$ ,  $\beta'_1=10.0$ ,

$$\beta'_2=10.0$$

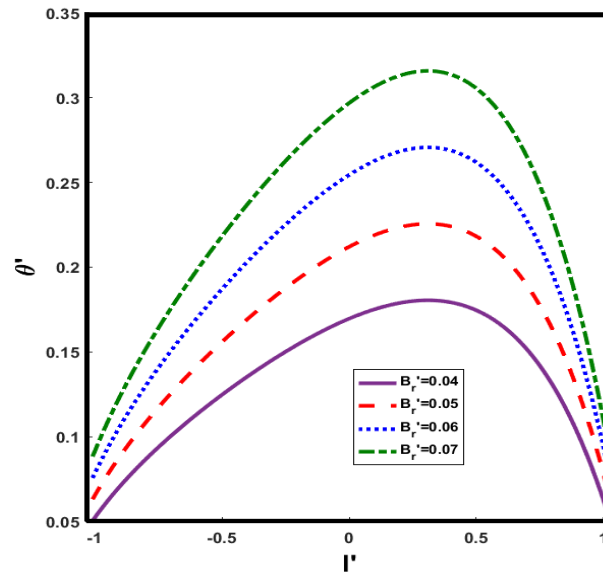


Figure 3. (b) Behavior of Temperature distribution for  $B_r'$  and  $M'=3.5$ ,  $\hat{k}=2.0$ ,  $\varepsilon'=0.1$ ,  $W_e'=0.01$ ,  $\beta_1'=10.0$ ,  $\beta_2'=10.0$

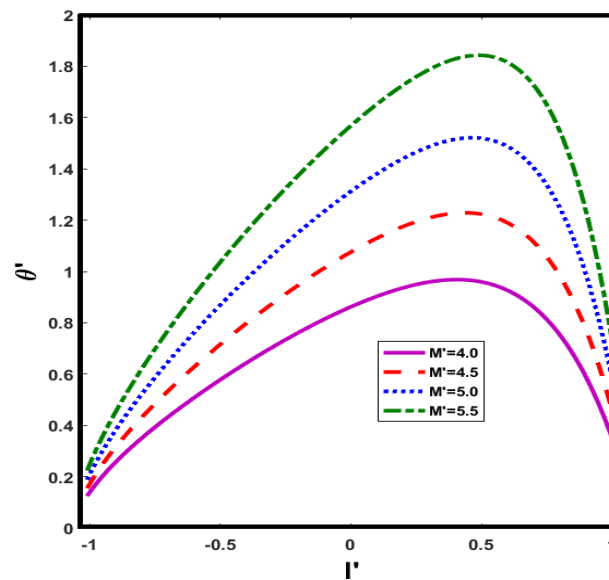


Figure 3. (c) Behavior of Temperature distribution for  $M'$  and  $\hat{k}=2.0$ ,  $\varepsilon'=0.1$ ,  $W_e'=0.01$ ,  $B_r'=0.1$ ,  $\beta_1'=10.0$ ,  $\beta_2'=10.0$

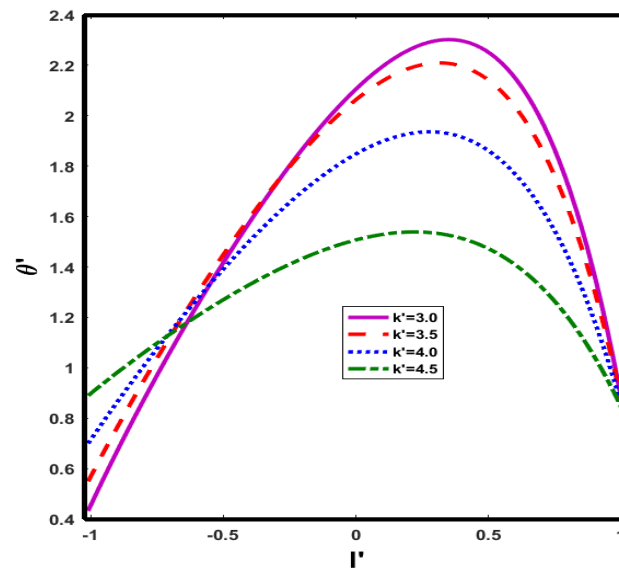


Figure 3. (d) Behavior of Temperature distribution for  $\hat{k}$  and  $M' = 3.5$ ,  $B_r' = 0.1$ ,  $\varepsilon' = 0.1$ ,  $W_e' = 0.01$ ,  $\beta_1' = 10.0$ ,  $\beta_2' = 10.0$

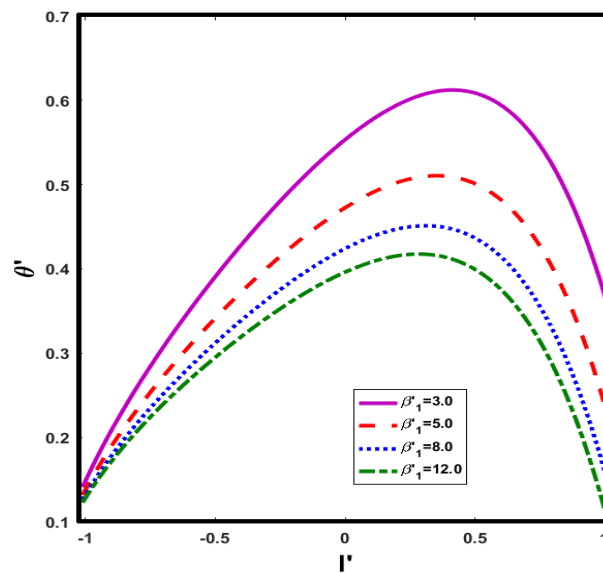


Figure 3. (e) Behavior of Temperature distribution for  $\beta_1' = 10.0$  and  $\beta_2' = 10.0$ ,  $M' = 3.5$ ,  $\hat{k} = 2.0$ ,  $\varepsilon' = 0.1$ ,  $B_r' = 0.1$ ,  $W_e' = 0.01$ ,  $\beta_2' = 7.0$

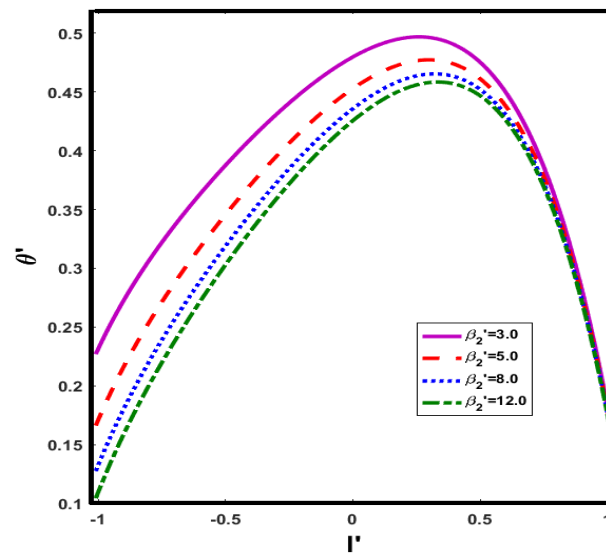


Figure 3. (f) Behavior of Temperature distribution for  $\beta_2'$  and  $M'=3.5$ ,  $\hat{k}=2.0$ ,  $\varepsilon'=0.1$ ,  $B_r'=0.1$ ,  $W_e'=0.01$ ,  $\beta_1'=7.0$

### (iii) Pumping characteristics

Influence of  $\hat{W}_e$ ,  $M'$  and  $\varepsilon'$  on pressure gradient is discussed and plotted in Fig 4(a)-4(c). Pressure gradient is maximum for small value of  $W_e'$ . One can observe enhancement in pressure gradient for large  $M'$  magnetic field (radial) in Fig 4(b). Similarly effect of  $\varepsilon'$  on pressure gradient can also be illustrated in Fig 4(c) by observing that pressure gradient is increasing while increasing  $\varepsilon'$  and has same behaviour as  $M'$  and finally it is resulted that electromagnetic forces are useful in the enhancement of pressure gradient.

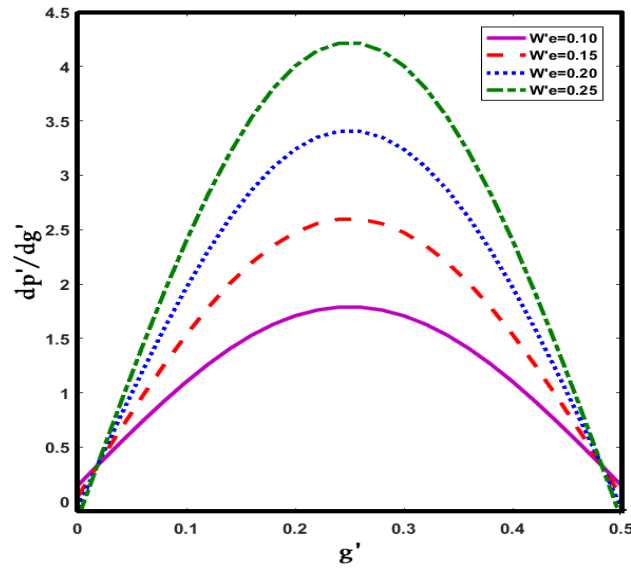


Figure 4. (a) Behavior of Pressure gradient for  $W'_e$  and  $M'=3.5$ ,  $\hat{k}=4.0$ ,  $\varepsilon'=0.1$ ,  $Q=0.01$

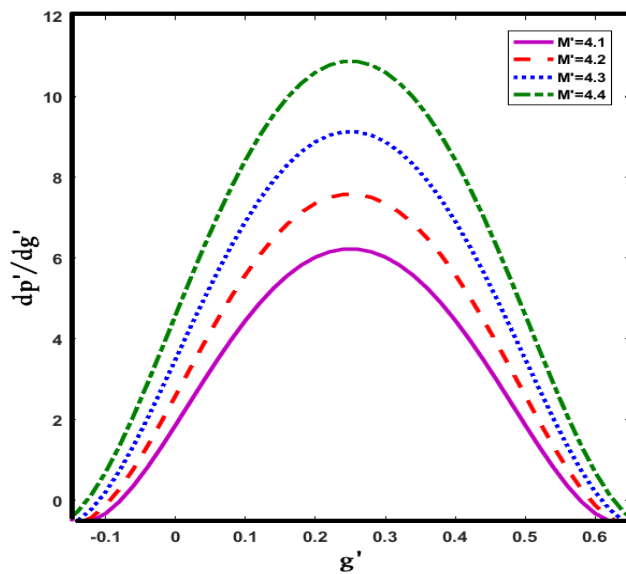


Figure 4. (b) Behavior of Pressure gradient for  $M'$  and  $W'_e=0.1$ ,  $\hat{k}=4.0$ ,  $\varepsilon'=0.1$ ,  $Q=0.01$

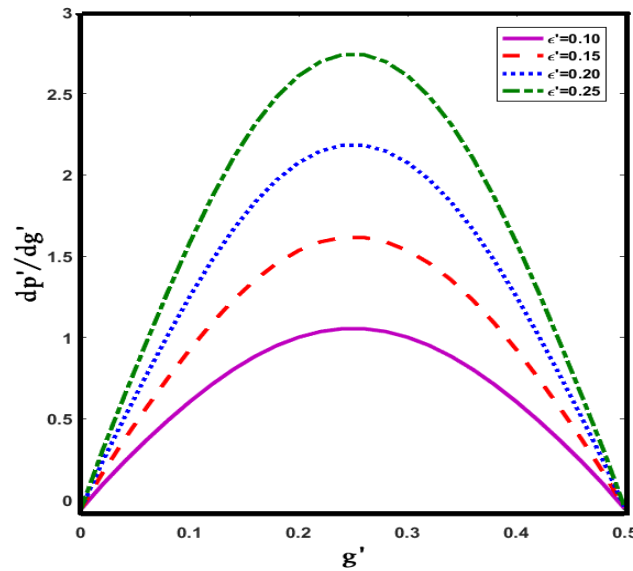


Figure 4. (c) Behavior of Pressure gradient for  $\varepsilon'$  and  $W_e'=0.1$ ,  $\hat{k}=4.0$ ,  $Q=0.01$

Figure 5. (a) - Figure 5. (d) is built to demonstrate the behavior of flow of heat or heat discharge for different material parameters at the upper wall of the channel. Coefficient of heat transfer or flow of heat is computed with the expression ( $Z' = \eta'_g \hat{\theta}(\eta')$ ). It is clearly observed in Figure 5. (a) that heat transfer coefficient  $Z'$  is increased by increasing value of  $W_e'$ . Flow of heat rate  $Z'$  behaves in a same way for  $B_r'$  in Figure 5. (b) as for  $W_e'$ . Figure 5. (c) and Figure 5. (d) shows the demonstration of the effects of Biot numbers on rate of flow of heat. It makes us visible that  $\beta_1'$  gives rise in the behaviour of  $Z'$  and falling attitude of  $\beta_2'$  respectively.



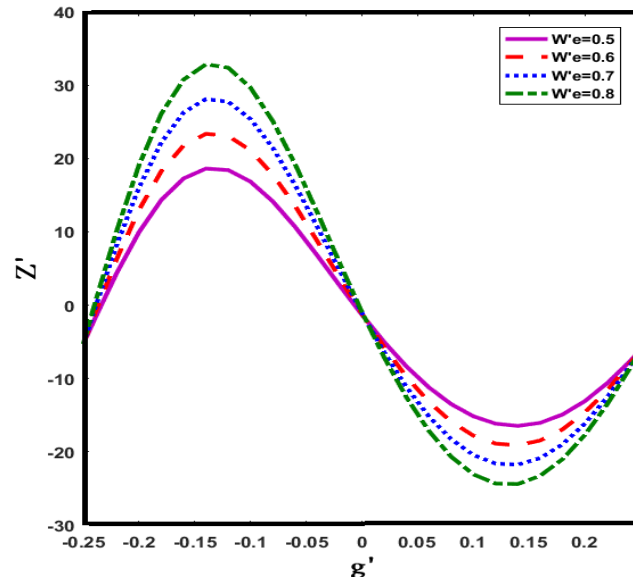


Figure 5. (a) Behavior of heat transfer for  $W'_e$  and  $M'=5, \hat{k}=3.0, \beta'_1=0.1, B'_r=0.2$

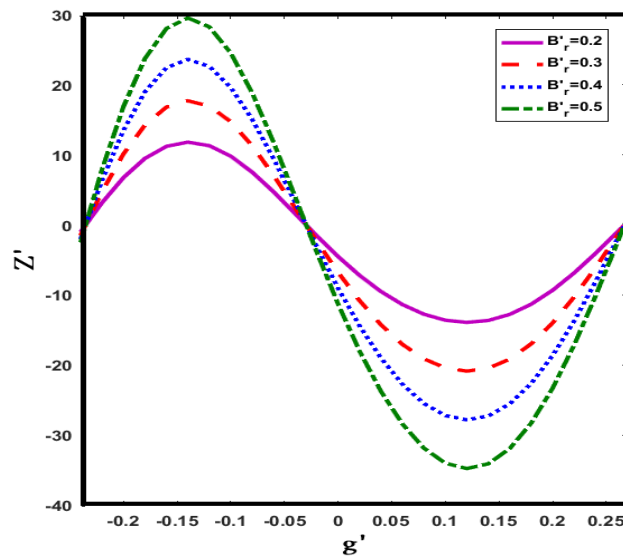


Figure 5. (b) Behavior of heat transfer for  $B'_r$  and  $M'=5, W'_e=0.9, \hat{k}=3.0, \beta'_1=0.1, \beta'_2=0.1$

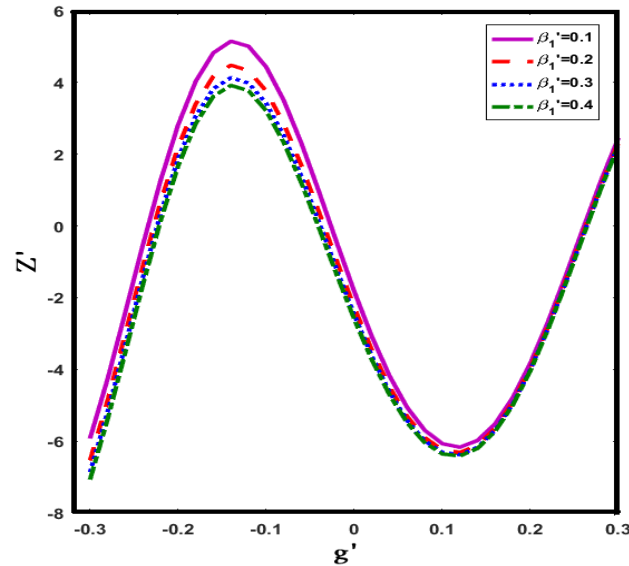


Figure 5. (c) Behavior of heat transfer for  $\beta_1'$  and  $M'=4$ ,  $W_e'=0.6$ ,  $\hat{k}=3$ ,  $\beta_2'=0.1$ ,  $B_r'=0.1$

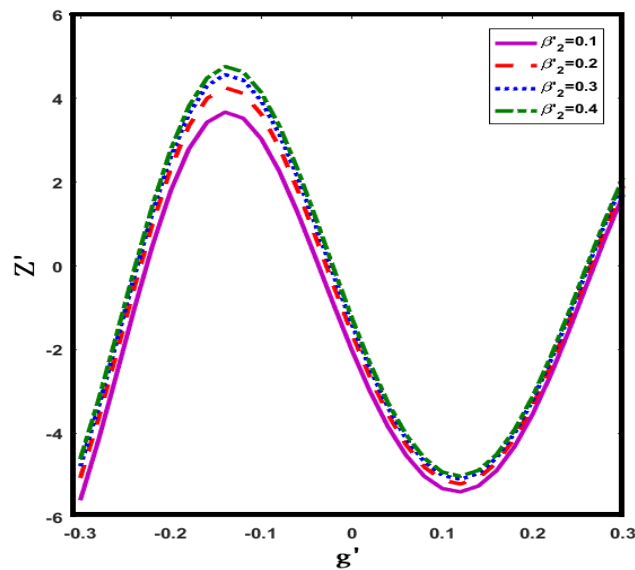


Figure 5. (d) Behavior of heat transfer for  $\beta_2'$  and  $M'=4$ ,  $W_e'=0.6$ ,  $\beta_1'=0.1$ ,  $B_r'=0.2$

#### (iv) Trapping

Another an interesting process of fluid motion is the trapping that is the shaping and formation of an interior circulation bolus of fluid which moves along the wave. There are some examples which illustrates this phenomenon are the food bolus movement in the gastrointestinal tract and movement of blood clot. Figs Figure 6. (a) - Figure 6. (f) are constructed to notice the deportment of trapped bolus. Figure 6. (a) and Figure 6. (a) shows the deportment of bolus for small values of  $W_e'$  and it is clearly observe that bolus size

is expanded with small value of  $W_e'$  Figure 6. (c) and Figure 6. (d) shows the size of trapped bolus for  $M'$  and it is also notice that bolus expanded with large values of  $M'$  Whereas Figure 6. (e) and Figure 6. (f) shows the behaviour of bolus with the change of  $\hat{k}$  (curvature parameter) and size of the trapping bolus increases with the increase of  $\hat{k}$ .

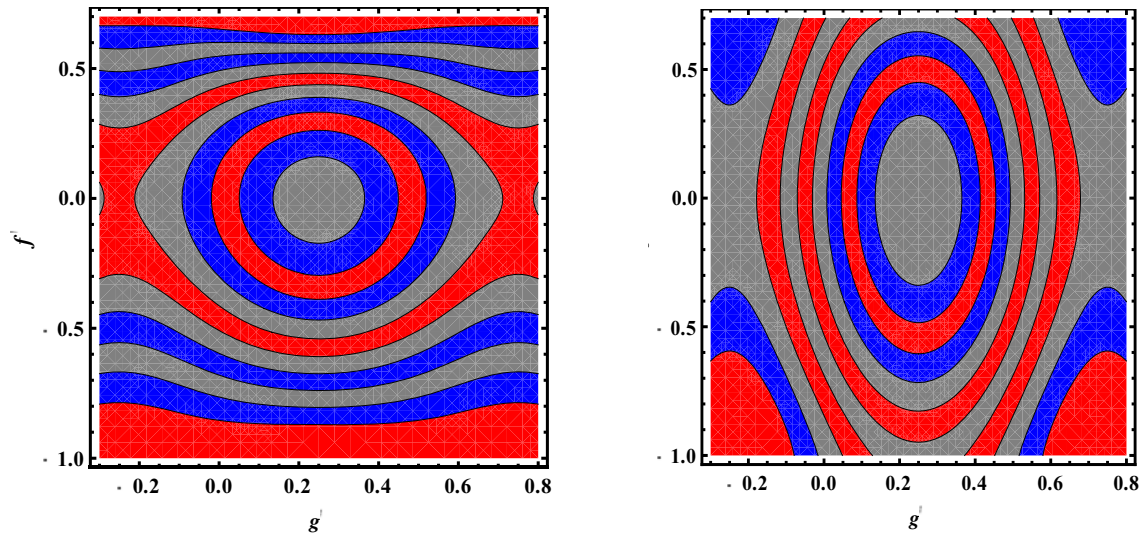


Figure 6. (a) - 6. (b) Trapped bolus for different values of  $W_e'$  with  $M'=5$ ,  $\hat{k}=3$ ,  $\epsilon'=0.1$ .

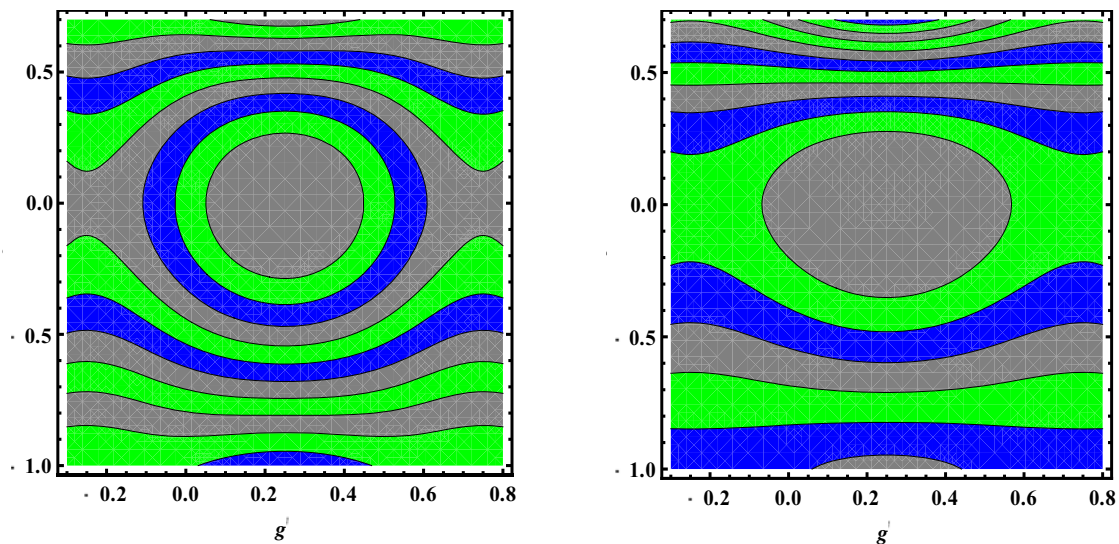


Figure 6. (c) - 6. (d) Trapped bolus for different values of  $M'$  with  $W_e'=0.01$ ,  $\hat{k}=3$ ,  $\epsilon'=0.1$ .

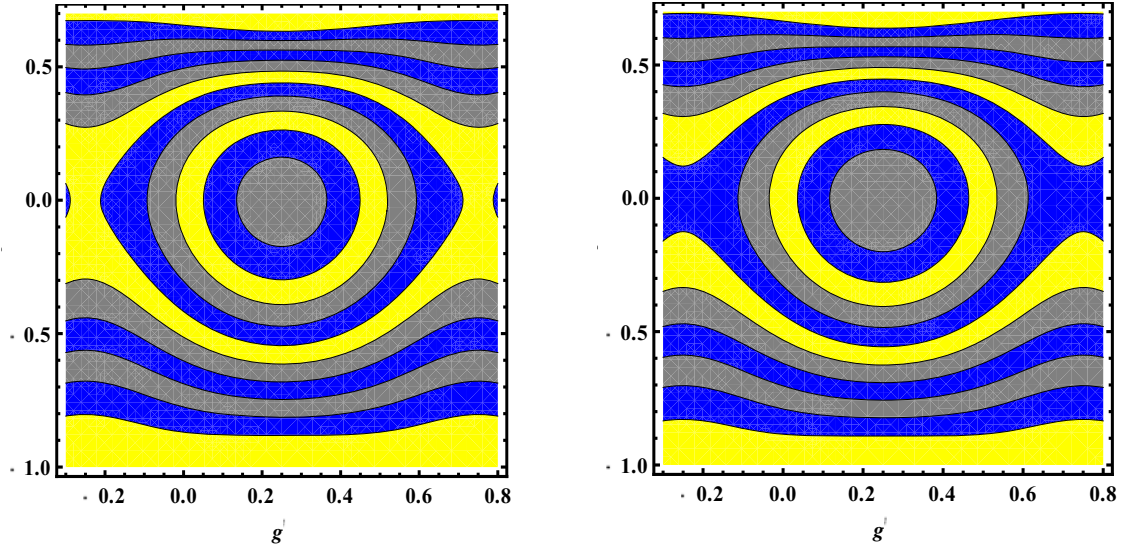


Figure 6. (e) - 6. (f) Trapped bolus for different values of  $\hat{k}$  with  $M' = 5$ ,  $W_e' = 0.01$ ,  $\varepsilon' = 0.1$ .

### (v) Conclusion

This research study presents the peristaltic transportation of Williamson fluid with MHD and Joule heating effects with convective heating in curved channel. The striking attention of the model on this regard are given as

1. Pressure gradient increases with increasing  $W_e'$ ,  $M'$  and  $\varepsilon'$ . While it decreases by increasing  $\hat{k}$  respectively.
2. Weissenberg number has same behavior for velocity and temperature profile
3.  $M'$  has opposite behaviour for velocity and temperature profile.
4. Curvature parameter  $\hat{k}$  also has opposite deportment for velocity and temperature distribution.
5. Oscillatory behaviour of Heat transfer coefficient  $Z'$  for all parameters.
6. Biot numbers  $\beta_1'$  and  $\beta_2'$  has decreasing behaviour on pressure gradient.

### Appendix

$$a_{11} = \frac{M'^2 (M'-1)^2 C_1^2 (l'+\hat{k})^{2M'+2}}{(M'+2)(3M'+2)} + \frac{M'^2 C_2^2 (M'-1)^2 (l'+\hat{k})^{-(2M'+2)}}{(3M'+2)(M'+2)}$$

$$a_{13} = \frac{2M'(M'^2-1)C_1C_2(l'+\hat{k})^{-2}}{(4-M'^2)} + \frac{2M'^2C_1^2(l'+\hat{k})^{2M'-1}}{(M'-1)(3M'-1)} - \frac{2M'^2C_1C_2(l'+\hat{k})^{-1}}{(1-M'^2)}$$

$$a_{14} = C_1(l'+\hat{k})^{M'} \ln(l'+\hat{k})$$

$$\begin{aligned}
a_{15} &= \frac{2M'^2 C_1 C_2 (l'+\hat{k})^{-1}}{(1-M'^2)} - \frac{C_2 (l'+\hat{k})^{-M'} \ln(l'+\hat{k})}{(4-M'^2)} - \frac{2M'^2 C_2^2 (l'+\hat{k})^{-2M'-1}}{(3M'+1)(M'+1)} \\
a_{16} &= \frac{M'^2 C_1^2 (l'+\hat{k})^{2(M'-1)}}{(M'-2)(3M'-2)} - \frac{M' C_2 (l'+\hat{k})^{-(M'+1)}}{(2M'+1)} - \frac{M' C_1 (l'+\hat{k})^{M'-1}}{2M'+1} - \frac{M' C_2 (l'+\hat{k})^{-(M'+1)}}{2M'+1} \\
a_{17} &= \frac{2M'^2 C_1 C_2 (l'+\hat{k})^{-2}}{(4-M'^2)} - \frac{2M' C_2 (l'+\hat{k})^{-(M'+1)}}{2M'+1} - \frac{2(l'+\hat{k})}{1-M'^2} - \frac{2M' C_1 (l'+\hat{k})^{(M'-1)}}{2M'+1} \\
a_{18} &= \frac{M'^2 C_2^2 (l'+\hat{k})^{-2}}{(4-M'^2)} + \frac{M'^2 C_2^2 (l'+\hat{k})^{-2(M'+1)}}{(3M'+2)(M'+2)} - \frac{M' C_1 (l'+\hat{k})^{M'-1}}{2M'-1} \\
a_{19} &= \frac{4M' C_1 (l'+\hat{k})^{\hat{M}+1}}{(2M'+1)} + \frac{2M' C_2 (l'+\hat{k})^{1-M'}}{(1-2M')} + \frac{2(l'+\hat{k})^2}{(4-M'^2)^2} \\
a_{20} &= \frac{2(l'+\hat{k})^2}{(4-M')^3} + \frac{(l'+\hat{k})^3}{(4-M'^2)^2 (1-M'^2)} \\
a_{21} &= \frac{(M'-1) C_2 (l'+\hat{k})^{-M'} \ln(l'+\hat{k})}{(4-M'^2)} - \frac{(M'-1) C_1 (l'+\hat{k})^{M'} \ln(l'+\hat{k})}{(4-M'^2)} \\
a_{22} &= \frac{C_2 (l'+\hat{k})^{-M'} \ln(l'+\hat{k})}{2(4-M'^2)} - \frac{C_1 (l'+\hat{k})^{M'} \ln(l'+\hat{k})}{2(4-M'^2)} - \frac{C_2 (l'+\hat{k})^{-M'} \ln(l'+\hat{k})}{(4-M'^2)} + \frac{C_1 (l'+\hat{k})^{M'} \ln(l'+\hat{k})}{2} \\
a_{23} &= \frac{(l'+\hat{k})^2}{2(4-M'^2)} - \frac{\hat{k}^3}{2M'^2} \\
b_{11} &= \frac{2C_1 C_2 M'^2 (l'+\hat{k})^{-2}}{4} \\
b_{12} &= \frac{2C_1 C_2 M'^4 (l'+\hat{k})^{-2}}{4} \\
b_{13} &= \frac{C_2^2 M'^2 (l'+\hat{k})^{-2(M'+1)}}{(2+2M')^2} \\
b_{14} &= \frac{C_1^2 M'^2 (l'+\hat{k})^{2M'-2}}{(2M'-2)^2} \\
b_{15} &= \frac{2C_1^2 M'^3 (l'+\hat{k})^{2M'-2}}{(2M'-2)^2}
\end{aligned}$$

$$b_{16} = \frac{C_1^2 M'^4 (l' + \hat{k})^{2M'-2}}{(2M'-2)^2}$$

$$b_{17} = \frac{2C_2 (1+M')(l' + \hat{k})^{-M'}}{M'(4-M'^2)}$$

$$b_{18} = \frac{2C_1 C_2 (1+M')M'^2 (l' + \hat{k})^{-2}}{4}$$

$$b_{19} = \frac{2C_1 C_2 M'^2 (M'-1)(l' + \hat{k})^{-2}}{4}$$

$$b_{20} = -\frac{2C_2 (l' + \hat{k})^{-M'}}{(4-M'^2)} + \frac{2C_1 (l' + \hat{k})^{M'}}{M'(4-M'^2)} - \frac{2C_1 (l' + \hat{k})^{M'}}{(4-M'^2)}$$

$$b_{21} = \frac{2C_2 (l' + \hat{k})^{-1}}{M'(4-M'^2)} - \frac{2C_1 (l' + \hat{k})^{\hat{M}}}{M'(4-M'^2)} - \frac{2C_1 (M'-1)(l' + \hat{k})}{M'(4-M'^2)}$$

$$b_{22} = \frac{(l' + \hat{k})^2}{4(4-M'^2)^2} - \frac{2C_2 \frac{dP_0}{dg'} (l' + \hat{k})^{-\hat{M}}}{\hat{M}(4-M'^2)}$$

$$c_{11} = -\frac{1}{4} + C_1 + \frac{5C_2}{8} + \frac{25C_1 (l' + \hat{k})^{-1}}{8} - \frac{7C_2 (l' + \hat{k})^{-1}}{4} + \frac{72(l' + \hat{k})^3}{36} - \frac{3C_2}{8}$$

$$c_{12} = \frac{6(l' + \hat{k})}{4} - \frac{C_1 (l' + \hat{k})}{2} - \frac{5C_2 (l' + \hat{k})}{4} - \frac{5C_1 (l' + \hat{k})^2}{32} - \frac{5C_1 (l' + \hat{k})^{-1}}{8} + \frac{3C_2 (l' + \hat{k})^{-1}}{8} + \frac{5C_1}{8}$$

$$c_{13} = -\frac{1}{8} + \frac{(l' + \hat{k})}{34} + \frac{5C_1}{16} - \frac{(l' + \hat{k})}{8} - \frac{3C_2}{16} - \frac{51(l' + \hat{k})^4}{(16)^2} + \frac{9(l' + \hat{k})}{8} - \frac{3(l' + \hat{k})^4}{128} - \frac{39(l' + \hat{k})^2}{192}$$

$$c_{14} = \frac{7(l' + \hat{k})^2}{64} + \frac{3C_2 (l' + \hat{k})}{32}$$

$$c_{15} = \frac{(l' + \hat{k})^2}{240} + \frac{(l' + \hat{k})^4}{1024} - \frac{(l' + \hat{k})^3}{64} + \frac{3(l' + \hat{k})^5}{1600} + \frac{3(l' + \hat{k})^2}{256} - \frac{(l' + \hat{k})^2}{128} + \frac{(l' + \hat{k})^2}{34}$$

$$c_{16} = -\frac{3C_2 (\ln(l' + \hat{k}))^2}{8} + \frac{12(\ln(l' + \hat{k}))^2}{4} + C_1 (\ln(l' + \hat{k}))^2 - \frac{5C_1 (\ln(l' + \hat{k}))^2}{8}$$

$$c_{17} = \frac{5C_1 (\ln(l' + \hat{k}))^2}{16} - \frac{3C_2 (\ln(l' + \hat{k}))^2}{16}$$

$$c_{18} = \frac{(l' + \hat{k})}{2} - \frac{(l' + \hat{k})^2}{4} + \frac{(\ln(l' + \hat{k}))^2}{4}$$

$$c_{19} = -3(l' + \hat{k})^2 - \frac{3(l' + \hat{k})^2}{4} - 6(l' + \hat{k}) + 4C_1(l' + \hat{k})^{-1} + \frac{10C_1C_2}{4} - 4C_1(l' + \hat{k})^{-1} + \frac{5C_2(l' + \hat{k})^{-1}}{2}$$

## References

- [1] Latham T (1966) Fluid motion in a Peristaltic Pump. MS thesis, MIT Cambridge MA.
- [2] Shapiro A, Jaffrin M, and Weinberg H (1969) Peristaltic pumping with long wavelength at low Reynolds number. *J. Fluid Mech.* **35** 799-825.
- [3] Hayat T, Farooq S, Ahmed B and Alsaedi A (2016) Characteristics of Convective heat transfer in the MHD peristalsis of Carreau fluid with Joule heating. *AIP Advances.* **6** 045302.
- [4] Akbar N, Nadeem S, and Khan Z (2014) Numerical simulation of peristaltic flow of a Carreau nanofluid in a asymmetric channel. *Alexandria Eng. J.* **53** 191-197.
- [5] Mustafa M, Abbasbandy S, Hina S and Hayat T (2014) Numerical investigation on mixed convective peristaltic flow of fourth grade fluid with Dufour and Soret effects. *J. Taiwan Inst. Chem. Eng.* **45** 308-316.
- [6] Mekheimer K, Abd Elmabound A and Abdellateef A (2013) particulate suspension flow induced by sinusoidal peristaltic waves through eccentric cylinders: thread annular. *Int. j. biomath.* **06** 1350026.
- [7] Hina S, Shit G, Ranjit N (2015) Peristaltic transport of MHD Flow and heat transfer in an asymmetrical channel: effects of variable viscosity, velocity-slip and temperature jump. *Alexandria Eng. J.* **54** 691-704.
- [8] Gad N (2014) Effects of Hall currents on peristaltic transport with complaint walls. *Appl. Math. Comput.* **235** 546-554.
- [9] Vafai K, Khan A, Sajjad S, and Ellahi R (2015) The study of peristaltic motion of third grade fluid under the effects of Hall current and heat transfer. *Z Naturforsch A.* **70** 281-293.
- [10] Rehman M, Akbar N, Haider A and Azam (2015) H Effects of heat sink/source on peristaltic flow of Jeffery fluid through a symmetrical channel. *Alexandria Eng. J.* **54** 733-743.
- [11] Hayat T, Abbasi F, Alsaedi A and Alsaedi F (2014) Hall and ohmic heating effects on the peristaltic transport of Carreau- Yasuda fluid in an asymmetric channel. *Z. Naturforsch A.* **69a** 43-51.
- [12] Awais M, Farooq S, Yasmin H, Hayat T and Alsaedi A (2014) Convective heat transfer analysis for MHD peristaltic flow of Jeffery fluid in an asymmetric channel. *Int. J. Biomath.* **7** 145002

- [13] Kothandapani M and Prakash J (2015) Effects of thermal radiation parameter and magnetic field on the peristaltic motion of Williamson nanofluids in a tapered asymmetric channel. *Int. J. Heat Mass Transf.* **81** 234-245.
- [14] Hameed M, Khan A, Ellahi R and Raza M (2015) Study of magnetic and heat transfer on the peristaltic transport of a fractional second grade fluid in a vertical tube. *Eng. Sci. Tech. Int. J.* **18** 496-502.
- [15] Saleem M and Haider A (2014) Heat and mass transfer on the peristaltic transport of non-Newtonian fluid with creeping flow. *Int. J. Heat Mass Trans.* **68** 514-526.
- [16] Hayat T, Tanveer A, Yasmin H and Alsaedi A (2014) Homogeneous-Heterogeneous reactions in peristaltic flow with convective conditions. *PLOS One.* (9) e113851.
- [17] Hina S (2016) MHD peristaltic transport of Eyring-Powell fluid with/mass transfer wall properties and slip conditions. *J. Mag. Mag. Mater.* **404** 148-158.
- [18] Akbar N, Raza M and Ellahi R (2015) Influence of induced magnetic field and heat flux with the suspension of carbon nanotubes for the peristaltic flow in a permeable channel. *J. Mag. Mag. Mater.* **381** 405-415.
- [19] Hayat T, Yasmin H and Alsaedi A (2015) Convective heat transfer analysis for peristaltic flow of power-law fluid in a channel. *J. Braz. Soci. Mech. Sci and Eng.* **37** 463-477.
- [20] Sato H, Kawai T, Fujita T and (2000) Okabe M Two dimensional peristaltic flow in curved channels. *Trans. Jpn. Soc. Mech. Eng. B.* **66** 679-685.
- [21] Mitra T, Prasad N (1973) On the influence of wall properties and Poiseuille flow in peristalsis. *J Biomech* **6** 68 1-693.
- [22] Davies C, Carpenter W (1997) Instabilities in a plane channel flow between compliant walls. *J Fluid Mech.* **352** 205-243.
- [23] Srivastava V, Srivastava L (1997) Influence of wall elasticity and poiseuille flow on peristaltic induced flow of a particle-fluid mixture. *Int J Eng Sci.* **35** 1359-1386.
- [24] Haroun M (2006) Effect of wall compliance on peristaltic transport of a Newtonian fluid in an asymmetric channel. *Math Prob Eng.* DOI:10.1155/MPE/2006/61475.
- [25] Radhakrishnamacharya G, Srinivasulu C (2007) Influence of wall properties on peristaltic transport with heat transfer. *Compt Rend Mecan.* **335** 369-373.
- [26] Muthu P, Kumar B, Chandra P (2008) Peristaltic motion of micropolar fluid in circular cylindrical tubes: Effect of wall properties. *Appl Math Model.* **32** 2019-2033.
- [27] Elnaby M, Haroun M (2008) A new model for study the effect of wall properties on peristaltic transport of a viscous fluid. *Commun Nonlinear Sci Numer Simul* **13** 752-762.



- [28] Hayat T, Javed M, Asghar S (2008) MHD peristaltic motion of Johnson–Segalman fluid in a channel with compliant walls. *Phys Lett A*. **372** 5026–5036.
- [29] Hayat T, Javed M, Ali N (2008) MHD peristaltic transport of Jeffery fluid in a channel with compliant walls and porous space. *Transp Porous Med*. **74** 259–274.
- [30] Ali N, Hayat T, Asghar S (2009) Peristaltic flow of a Maxwell fluid in a channel with compliant walls. *Chaos Solitons Fractals*. **39** 407–416.
- [31] Kothandapani M, Srinivas S (2008) On the influence of wall properties in the MHD peristaltic transport with heat transfer and porous medium. *Phys Lett A*. **372** 4586–4591.
- [32] Srinivas S, Gayathri R and Kothandapani M (2009) The influence of slip conditions, wall properties and heat transfer on MHD peristaltic transport. *Comput Phys Commun*. **180** 2115–2122.
- [33] Srinivas S, Kothandapani M (2009) The influence of heat and mass transfer on MHD peristaltic flow through a porous space with compliant walls. *Appl Math Comput*. **213** 197–208.
- [34] Hayat T, Hina S (2010) The influence of wall properties on the MHD peristaltic flow of a Maxwell fluid with heat and mass transfer. *Nonlinear Anal: Real World Appl*. **11** 3155–3169.
- [35] Sato H, Kawai T, Fujita T and Okabe M (2000) Two dimensional peristaltic flow in curved channels. *Trans The Japan Soc Mech Eng B*. **66** 679–685.
- [36] Ali N, Sajid M and Hayat T (2010) Long wavelength flow analysis in a curved channel. *Z Naturforsch A*. **65** 191–196.
- [37] Ali N, Sajid M and Javed T (2000) Heat transfer analysis of peristaltic flow in a curved channel. *Int J Heat Mass Transf*. **53** 3319–3325.
- [38] Ali N, Sajid M, Abbas Z and Javed T (2010) Non-Newtonian fluid flow induced by peristaltic waves in a curved channel. *Europ J Mech- B/Fluids* 29:387–394.
- [39] Hayat T, Javed M, Hendi A (2011) Peristaltic transport of viscous fluid in a curved channel with compliant walls. *Int J Heat Mass Transf*. (2011) **54** 1615–1621.
- [40] Hayat T, Hina S, Hendi A and Asghar S (2011) Effect of wall properties on the peristaltic flow of a third grade fluid in a curved channel with heat and mass transfer. *Int J Heat Mass Trans*. **54**:5126–5136.
- [41] Hina S, Hayat T, Asghar S (2012) Peristaltic transport of Johnson–Segalman fluid in a curved channel with wall properties. *Nonlinear Anal: Model Control*. **17** 297–311.
- [42] Hina S, Hayat T, Alsaedi A (2012) Heat and mass transfer effects on the peristaltic flow of Johnson–Segalman fluid in a curved channel with compliant walls. *Int J Heat Mass Transf*. **55** 3511–3521.

- [43] Hina S, Mustafa M, Hayat T and Alsaedi A (2013) Peristaltic flow of pseudoplastic fluid in a curved channel with wall properties. *J Appl Mech Trans ASME*. **80** 024501 (doi:10.1115/1.4007433).
- [44] Hina S, Mustafa M, Hayat T and Alsaedi A (2014) Peristaltic motion of third grade fluid in curved channel. *Appl Math Mech-Engl Ed*. **35** 73–84.
- [45] Hina S, Mustafa M, Abbasbandy S, Hayat T and Alsaedi A (2014) Peristaltic motion of nanofluid in a curved channel. *J Heat Transf -Trans ASME*. **136** 052001 (doi:10.1115/1.4026168).
- [46] Khan M, Hina S, Al-Hina A and Dutta J (2014) Visible light photocatalysis of mixed phase zinc stannate/zinc oxide nanostructures precipitated at room temperature in aqueous media *Ceramics International*.
- [47] Baruah S, Khan M, J Dutta (2015) Pollutants in Buildings, *Water and Living Organisms*.
- [48] Baruah S, M Khan and Dutta J (2016) Perspectives and applications of nanotechnology in water treatment - *Environmental chemistry letters*.
- [49] Iftikhar N, Rehman A, Sadaf H and M Khan (2018) Impact of wall properties on the peristaltic flow of Cu-water nano fluid in a non-uniform inclined tube. *Int J Heat Mass Transf*. **125** 772-779